Sliding Mode Control of VTOL System

IOP Conf. Series: Materials Science and Engineering **561** (2019) 012069 doi:10.1088/1757-899X/561/1/012069

Sliding Mode Control of VTOL System

Jerry Jacob, S Selva Kumar

Department of Electrical and Electronics Engineering,
Amrita School of Engineering, Coimbatore, Amrita VishwaVidyapeetham, India

Abstract. QUANSER QNET 2.0 Vertical Take Off and Landing (VTOL) system is a hardware device setup developed by National Instruments to study flight dynamics and vertical take-off and landing control. It has a DC Motor fan and adjustable counter weight. This is used exclusively for NI-ELVIS platform and LabVIEW software. The LabVIEW software is used to identify the model of the system by the method of best fit. The obtained second order model is tested for the open loop response using MATLAB SIMULINK. The various control methods like Proporional+Integral+Velocity (PIV) and Sliding Mode Control (SMC) are used to find the response of the system. It is found that the sliding mode controller provides better results compared to the PIV controller. Along with this, the actuator control is done using PI controller and it's response along with the system is analyzed and compared for both PIV and Sliding Mode Controller.

1. Introduction

Vertical Take-off and Landing aircrafts are those which possess the ability to hover, take –off and land vertically. Classifications vary from fixed wing air-craft to helicopters. Some VTOL aircrafts operates in other modes as well. These are CTOL (Conventional Take-Off and Landing), STOL (Short Take-Off and Landing) and STOVL (Short Take-Off and Vertical Landing). In a flight or airplane there are three types of motion which affect the stability and control. These are yaw, roll and pitch. Roll is the rotation of the aircraft around the front-to-back axis. Pitch is the rotation of the airplane from side-to-side axis. Whereas, the rotation around the vertical axis is known as yaw.

The salient features of the QUANSER QNET 2.0 VTOL system are high speed DC motor with a safety guard, a propeller assembly, a digital tachometer, a current sensor, a PWM amplifier, optical encoders to find the position of the arm and a protective cover. It has a built in Peripheral Component Interconnect (PCI) connector which interfaces it to NI-ELVIS. This system is fully compatible with LabVIEW software. The mass of the counter-weight is 258g. The resolution of the encoder is 0.176°/count. The peak current of the amplifier is 2.5A, while the continuous current is 0.5 A. The output voltage of the amplifier is ±24V with 42% duty cycle. The QNET VTOL is designed for indoor use only. The temperature which it can withstand is from 5° C to 40 ° C. It can bear up to an altitude of 2000 m. The maximum relative humidity of 80% at 31°C which decreases linearly to 50% relative humidity at 40°C. The mains supply voltage is ±10V of the nominal voltage. The maximum transient overvoltage is 2500V. The pollution degree of the device is 2.

The PI controller is used for the actuator of the QUANSER QNET 2.0 VTOL system. The actuator regulates the input current drawn by the system. Generally, the system uses the PIV controller. But the sliding mode control is incorporated instead of PIV and analysis is done.

2. Literature Survey

Peter Martin *et.al.*[1] has done the basic modeling of the QUANSER QNET 2.0 VTOL system. Through this, the second order transfer function of the VTOL system can be found out. Also Peter Martin *et.al.*[2] had done the white box model of the system. Various parameters of the VTOL system especially for the DC Motor fan and other components are present and the respective transfer function can be derived. S Mondal and C Mahanta [3] had proposed a second order sliding mode controller in

order to stabilize the VTOL system. S Anoop and K.R.Sharma [4] had done simulation studies based on the QUANSER QNET 2.0 VTOL system for Model Predictive Controller (MPC). The simulation of the MPC is compared to that of the conventional PID controller. The authors [5] had done an altitude control of a VTOL tail sitter Unmanned Aerial Vehicle (UAV). The pitch as well as the roll control of the UAV is done. J Zhang *et.al.* [6], had designed a UAV with a platform structure for multi-rotors and fixed wing rotors (FW) on conventional control surface. The mathematical model of the UAV is discussed and control methodologies are implemented in this work. S. Niwa and I. Sugiura [7] discussed about acontrol methodology for VTOL aircraft supported by ducted fan. Various problems like stability, control and fuel efficiency were solved in this work. The authors [8] had implemented a linear optimal design approach with multi-variable control laws in VTOL aircrafts. A. Yang and Y. Wang [9] presented a new type of vertical take-off and landing (VTOL) aircraft which alters the three elements of thrust. A plan for a non-linear segmentation is proposed and the degree of correctness is found through numerous simulations. R.K.R.Ana*et.al.*[10] had discussed about a new control design of the PIV controller. The compensator and controller are made using the Eigen value assignment method. The authors [11] had designed a sliding mode controller for a boost converter.This paper presents a model identification procedure for the VTOL system and compares the system response for different controllers likePIV and SMC. Also, a PI controller is tuned for the actuator and the overall system response is studied and compared for PIV and SMC incorporated in the VTOL system.

3. Theoretical Background

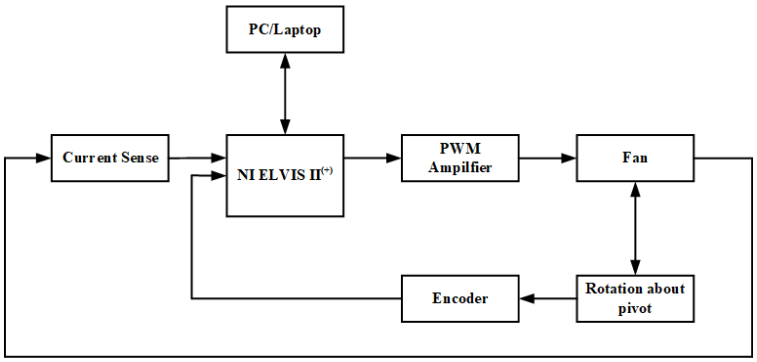

Figure 1. Block Diagram of VTOL System

NI-ELVIS is known as NI Educational Laboratory Virtual Instrumentation Suite. It is an engineering device used by students and professionals in academia. Figure 1.shows the interactions between NI-ELVIS board and the VTOL system. The VTOL system consists of the PWM amplifier, fan, encoder and the current sensor. The PWM amplifier is used to power on the high speed DC fan motor. As the fan operates the system moves about the pivot. The encoder is used to find the position of the VTOL system. A current sensor is used in order to measure the current taken by the PWM amplifier.

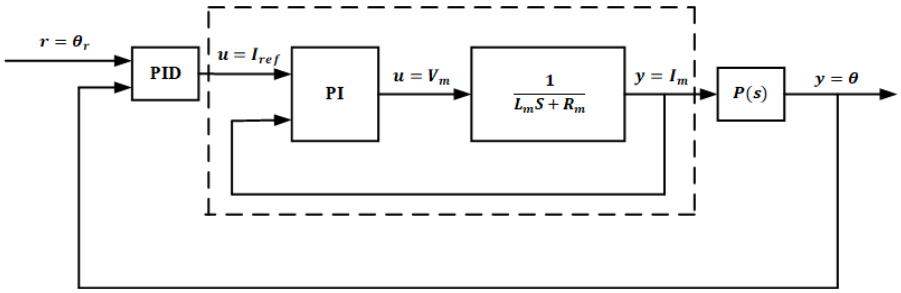

Figure 2. Cascade Control of a QUANSER QNET 2.0 VTOL System

Figure 2 depicts the cascade control of the QUANSER QNET 2.0 VTOL system. It is divided into two subsystems: the voltage-current dynamics of the actuator i.e. the motor and the position dynamics of the VTOL. The controller in the inner loop is designed to control or regulate the current of the high speed fan DC motor. The reference current is generated from the outer loop using the controller present in the outer loop. The outer loop is used to control the pitch of the system.

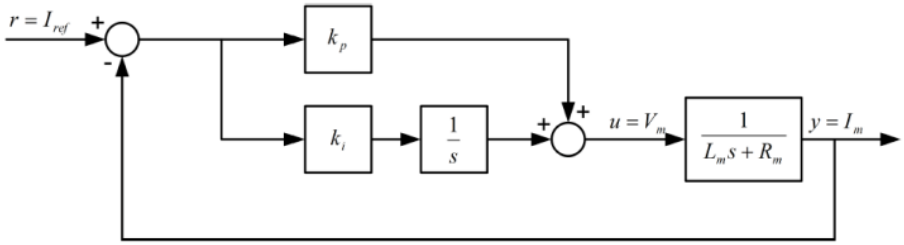

Figure 3.PI Control of the High Speed DC Motor

Figure 3 illustrates the PI control of the high speed DC motor i.e. the actuator. This is required when the actuator of a system has slower dynamics. PI controller is used in order to regulate the flow of the current to the entire system. This makes the actuator dynamics very small making the overall system simpler.
Equation (1) shows the voltage-current relationship of the DC motor actuator,

$$v_m = R_m i_m + L_m \frac{di_m}{dt} \tag{1}$$

The voltage across the motor is v_m, i_m current drawn by the motor with resistance $R_m$and inductance of the motor is L_m.
Equation (2) shows the voltage-current relation in the transfer function form,

$$I_m = \frac{V_m}{sL_m + R_m} \tag{2}$$

The transfer function of the system has V_m i.e. voltage induced to the motor as the input to the actuator and I_m i.e. the output current to be induced to the system as output.

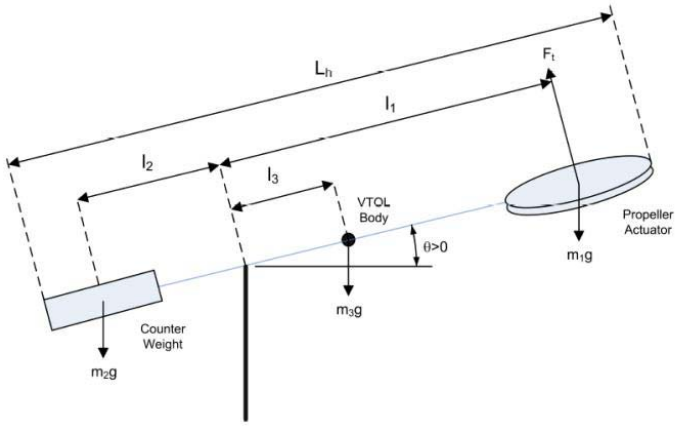

Figure 4. Free Body Diagram of VTOL System

Unlike the DC motor, the VTOL system can be characterized by a second order equation. The VTOL system consists of propeller actuator, VTOL body and counter weight. Fig 4 shows the free body

diagram depicting these parts. Equation (3) gives the transfer function of the VTOL system [1] which is derived from the free body diagram.

$$P(s) = \frac{K_t}{J\left(s^2 + \frac{B}{J}s + \frac{K}{J}\right)} \quad (3)$$

where, K_t-thrust current torque constant Nm/A
J -moment of inertia in kgm^2
B -viscous damping in Nm/(rad/s)
K-stiffness of the VTOL system in Nm/rad

Referring [1] and [2] the parameters of the transfer function of the VTOL system were found as in Table 1.

Table 1. Parameters of QUANSER QNET VTOL System

S.No	Parameters	Values
1.	J	0.0045kgm^2
2.	B	0.002 Nm/(rad/s)
3.	K_t	0.1562 Nm/A
4.	R_m	40.2 Ω
5.	L_m	2 H
6.	m_1	258g
7.	m_2	127g
8.	l_1	72.5mm
9	l_2	155mm
10.	K	0.0218 Nm/rad

Using Table 1, the transfer function of the VTOL system can be found out using equation (3). Equation (4) shows the transfer function of the system when the values mentioned in Table 1 are assigned,

$$P(s) = \frac{34.71}{s^2 + 0.444s + 4.84} \quad (4)$$

Equation (5) shows the transfer function of actuator,

$$I_m(s) = \frac{1}{2s + 40.2} \quad (5)$$

4. Controllers for VTOL system

PI controller is used for the control of the actuator or the high speed DC motor fan. It is a very popular controller used in process control industries. PI controller is represented by Equation (6),

$$u = K_p e + K_i \int e.dt \quad (6)$$

Where,K_P - Proportional Gain constant
K_i - Integral Gain constant
e - Error

The proportional gain, K_P multiplies the error and it drives the output proportional to error. Integral gain, K_i decreases the rise time, increases overshoot and settling time but it eliminates steady state error.

PIV controller is used to control the pitch of the QUANSER QNET 2.0 VTOL system. It has two components i.e. the feed forward control used to add auxiliary velocity and in some cases acceleration signals are added to the servo loop in order to improve command tracking. These components play a crucial role in rejecting disturbances. PIV controller is represented by Equation (7),

$$U(s) = K_p E(s) + \frac{K_i}{s} E(s) - K_v \times \frac{Ns}{s+N} \qquad (7)$$

where , K_P - Proportional Gain constant
K_i - Integral Gain constant
K_v-Velocity constant
N-constant of the feed forward control
$E(s)$ - Error in s domain

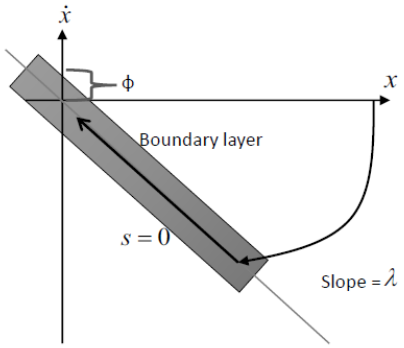

Figure 5. Sliding Surface or Manifold of the Sliding Mode Controller

Like the PIV controller, there also exist three parameters for sliding mode control. The parameters are sliding mode gain, K, sliding mode slope, λ and sliding mode thickness, ϕ. These parameters are used to control the system according to the sliding manifold or surface shown in Figure 5. As the sliding mode thickness, ϕ increases, the chattering of the system response decreases. However, the steady state error slightly increases as the thickness, ϕincreases.
Equation (8) gives the function of the sliding surface,

$$s = \lambda e + \dot{e} \qquad (8)$$

The sliding mode function, s is the sum of the products of slope, λ and error, e and derivative of error. The derivative of the error is needed to do the tracking of a set point.
Equation (9) shows the switching function of the sliding mode controller,

$$Switching\ Function = \begin{cases} sign(s)\ for |s| > \phi \\ \dfrac{s}{\phi} \qquad for |s| < \phi \end{cases} \qquad (9)$$

When $|s|$ is greater thanϕ, the signum function of s is considered. Otherwise the function chosen is s/ϕ. This function is taken to derive the output of the controller.
Equation (10) gives the output of the sliding mode controller,

$$Output = -(\dot{e} - K \times Switching\ Function) \qquad (10)$$

The output of the controller is the sum of the product of sliding mode gain, K and switching function and derivative of error. This is introduced to the plant in order to reach the set point at the earliest.

5. Model Identification

Figure 6. Hardware Setup of VTOL System with Interface

The QUANSER QNET 2.0 VTOL is fixed to the NI-ELVIS hardware interface board. Fig 6 shows the hardware setup of QUANSER QNET2.0 VTOL system. The NI-ELVIS board is connected to a PC/Laptop via a USB cable. The software used for the model identification of the VTOL system is LabVIEW 2015. LabVIEW is known as Laboratory Virtual Instrumentation Engineering Workbench. The unique feature of LabVIEW compared to other software is that it makes use of graphical programming or G-programming. This allows users to access the blocks required for a particular function. LabVIEW consists of two windows: front panel and block diagram. Front panel is where the user can see the results. On the other hand, block diagram is used to do the graphical coding.

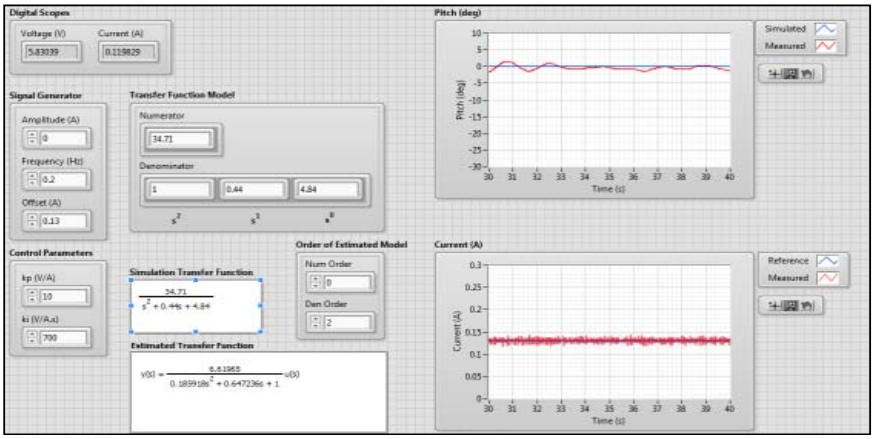

Figure 7. Front Panel of VTOL System to find Balancing Current.

Initially the transfer function derived in equation (4) is used in Figure 7. A signal of amplitude 0 A, frequency of 0.2 Hz and offset of 0.13 A is introduced into the system under use. It is observed that the VTOL system remains still in the horizontal direction i.e. the pitch of the system is at 0°. Hence the balancing current is found to be at 0.13 A.

Using this balancing current, the model identification of the VTOL system can be found out. A signal of amplitude 0.02A, frequency of 0.2 Hz and offset of 0.13 A is used in this case to find out the model. The transfer function from Equation (4) is used initially to find the best fit response. However, it is observed that the best fit condition does not occur when equation (4) is used in the front panel. Hence, it cannot be used.

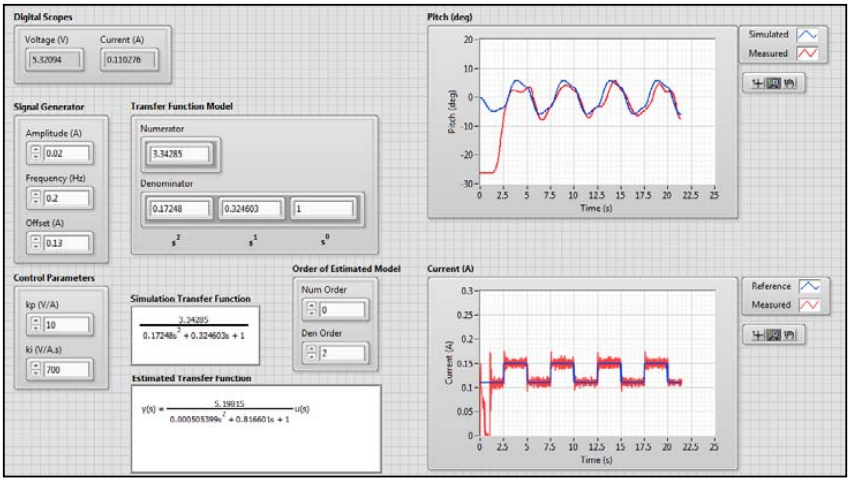

Figure 8. Model with Best Fit

The estimated transfer function is found out in the front panel. On further iterations, the transfer function of the system which has the best fit is found out. The response is depicted in Figure 8. Equation (11) gives the best fit model of the system,

$$P(s) = \frac{3.34285}{0.17284s^2 + 0.324603s + 1} \tag{11}$$

On further simplification, Equation (12) is found out,

$$P(s) = \frac{19.36}{s^2 + 1.8819s + 5.7977} \tag{12}$$

This transfer function in Equation (12) is used for simulations and analysis.

6. Controller Implementation

The simulation of VTOL system with the PIV controller is done and then compared with that of the sliding mode controller. The Control System tuner app is used to tune the parameters K_p, $K_i$and K_v. The feed forward control constant, N is considered as 25. Hence the transfer function for the velocity parameter is shown in Equation (13),

$$T_k(s) = \frac{25s}{s + 25} \tag{13}$$

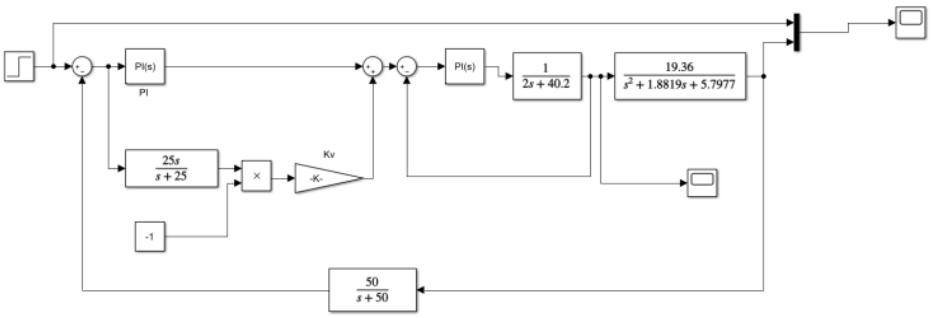

Figure 9. Block Diagram of PIV Controller with VTOL System

Figure 9 shows the block diagram of the PIV controller with the QUANSER QNET 2.0 VTOL system. A step signal is introduced to the system. The PIV controller consists of the PI block and a gain block, K_v. This is used to control the outer loop of the system. The actuator is controlled by the PI controller i.e. the inner loop. The parameters of the PIV controller are tuned using the Control System tuner app, whereas the PI control of the actuator is done by using the auto tuning method which is available in the MATLAB SIMULINK software. Using these tuning methods the parameters are K_p= 0.5666, K_i = 2.5065 and K_v= -0.4449 for the outer loop. While for the inner loop the parameters are K_p= 100.8318 and K_i = 7507.5568.

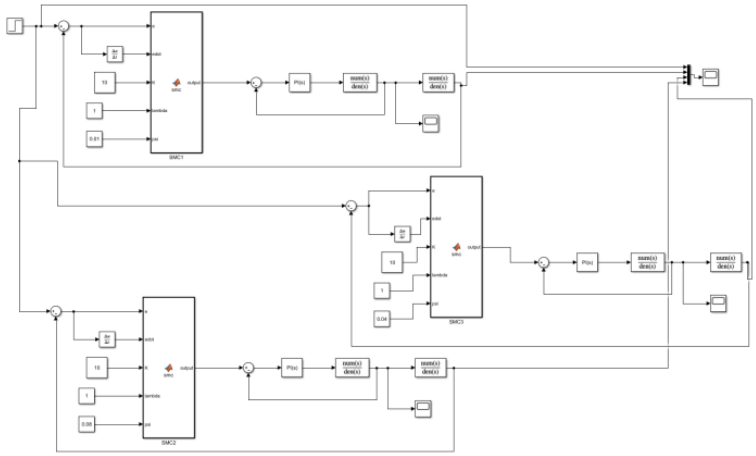

Figure 10. Block Diagram of SMC with VTOL System

Figure 10 shows the sliding mode control of the VTOL system. Like the PIV control, a step function is introduced to the system as the input. The MATLAB function is used to design the sliding mode controller. Instead of the PIV controller, the sliding mode controller acts as the controller here for the outer loop. The PI control of the actuator remains the same in this case. On using the trial and error method for sliding mode controller for the outer loop, the parameters are found to be K=10, λ=1 and ϕ=0.01, 0.04 or 0.08. While using the same tuning methodology for PI controller, the parameters are found to be K_p=1 and K_i=2.

7. Results

The VTOL system is simulated using SIMULINK for two control methodology namely PIV control and sliding mode control. The results were discussed for a step input variation to observe the change in the response of the system. Various observations and corresponding inferences were discussed.

Figure 11. Actuator Response of PIV control for VTOL System

Figure 11 shows the actuator response of the system under PIV controller. Initially, the system at 0.02 seconds will reach a peak of 4 V. However, at approximately 0.2 seconds the voltage reaches a low of -1 V. The system settles at 0.15 A with some chattering at approximately 0.6 seconds.

Figure 12. Response of VTOL System with PIV Controller

Figure 12 illustrates the response of the PIV control of the VTOL system. A step response of 0.5 is given to the system. It is observed that the peak of the response is at 0.52° when the time is approximately 0.3 seconds. After 0.3 seconds, uneven oscillations occur in the system. The system settles at 12 seconds for 2% tolerance band. However, the system which is under the PIV control will have some chattering effect as the system reaches the tolerance band.

Figure 13. Actuator Response of SMC for VTOL System

Figure 13 depicts the actuator response using PI controller where K_p=1 and K_i=2. However, it is observed that the sliding mode thickness, ϕaffects the response of the actuator. Basically sliding mode thickness is used to reduce the chattering effect present in the system. Table 2 shows the peak, settling time and the voltage at which the system settles for different sliding mode thicknesses.

Table 2. Time Domain Specifications for Different Sliding Mode Thicknesses

S.No	Sliding mode thickness	Peak overshoot	Peak time	Settling time	Settling point
1.	0.01	0.286 V	0.15s	No settling time	No settling point
2.	0.04	0.282 V	0.15s	4.4s	0.1495 A
3.	0.08	0.274 V	0.13s	4.4s	0.1494A

From Table 2, it is understood that when the sliding mode thickness, ϕ is less, the system fails to settles and oscillates unevenly. But as the thickness, ϕ increases the actuator regulates itself to a value and remains to be in settled state. It is also observed that there exists a settling time at which the actuator settles as ϕ increases. The peak overshoot of the system increases as the sliding mode thickness is decreased.

Figure 14. Response of VTOL System with SMC

Figure 14 depicts the response of the system using sliding mode control. A step function of 0.5° is introduced to the VTOL system. The sliding mode thicknesses, ϕ used in this system are 0.01, 0.04 and 0.08 along with sliding mode gain, K=10 and sliding mode slope, λ=1. Generally, the system settles at about 8.5 seconds. The chattering present in the actuator response can be viewed in system response. Table 3 gives the peak overshoot, peak time, settling time and settling point in the system.

Table 3. Chattering and settling points for various sliding mode thicknesses

S.No	Sliding mode thickness	Chattering	Settling point
1.	0.01	More	Between 0.501° and 0.485°
2.	0.04	Less	About 0.4995°
3.	0.08	Least	About 0.4987°

Table 3 shows that when sliding mode thickness is less, chattering is more. When ϕ=0.01, the steady state error may be difficult to find out due to the chattering present. As ϕ increases to 0.04, the steady state error is -0.0005°. On increasing further to 0.08, the steady state error is found to be -0.0013°. The settling time for the system with any sliding mode thickness, ϕ is 8 seconds. Therefore, it can be inferred that the steady state error decreases with increase in the sliding mode thickness, ϕ.

8. Conclusion

The QUANSER QNET 2.0 VTOL system was studied and analyzed with different controllers. The mathematical model of the system was identified using LabVIEW. The obtained mathematical model is considered for the simulation studies The PIV and sliding mode controllers are implemented for the VTOL system model and results were compared and analyzed for a step change in input. SMC controller with different sliding mode thickness and its effect on the system response were studied. It is inferred that the peak overshoot and settling time are found to be lesser for sliding mode controller compared to PIV controller. From results obtained, it is understood that sliding mode control produces better results compared to PIV controller for a VTOL system.

References

[1] Peter Martin *et.al* 2015 *INSTRUCTOR WORKBOOK- QNET 2.0 VTOL Board for NI-ELVIS* (QUANSER).

[2] Peter Martin *et.al* 2015 *USER MANUAL- QNET 2.0 VTOL Board for NI-ELVIS* ,QUANSER**3** 18.

[3] S. Mondal and C. Mahanta 2013 *Observer based sliding mode control strategy for vertical take-off and landing (VTOL) aircraft system* (Melbourne) ,pp.1-6.

[4] S. Anoop and K. R. Sharma 2018 *Model predictive control: Simulation studies for the implementation on vertical take-off and landing labprototype* Procedia Computer Science, vol. 143, pp. 663-670.

[5] S. Verling, B. Weibel, M. Boosfeld, K. Alexis, M. Burri and R. Siegwart 2016 *Full Attitude Control of a VTOL tailsitter UAV* 2016 IEEE International Conference on Robotics and Automation (ICRA)(Stockholm), pp. 3006-3012.

[6] J. Zhang, Z. Guo and L. Wu 2017 *Research on control scheme of vertical take-off and landing fixed-wing UAV* 2017 2nd Asia-Pacific Conference on Intelligent Robot Systems (ACIRS),(Wuhan) , pp. 200-204.

[7] S. Niwa, I. Sugiura 1987 *An Automatic Flight Control System for VTOL Aircraft Supported by Ducted Fans* IFAC Proceedings Volumes, vol 20, issue 5, part 6, ,pp 145-150.

[8] R. F. Stengel, J. R. Broussard and P. W. Berry 1976 *Digital controllers for VTOL aircraft* 1976 IEEE Conference on Decision and Control including the 15th Symposium on Adaptive Processes, (Clearwater)(FL, USA) , pp. 1009-1016.

[9] A. Yang and Y. Wang 2017 *A new VTOL aircraft*2017 36th Chinese Control Conference (CCC*)*, (Dalian), pp. 6213-6218

[10] R. K. R. Ana, N. Choudhary, J. S. Lather and G. L. Pahuja 2014 *PIV and lead compensator design using Lambert W function for rotary motions of SRV02 plant* 2014 IEEE 10th International Colloquium on Signal Processing and its Applications *(*Kuala Lumpur) , pp. 266-270.

[11] V. Vijayakumar, R. Divya, and A. Vivek 2014 *Sliding mode controlled quadratic boost converter* International Conference on Computation of Power, Energy, Information and Communication (ICCPEIC)(Chennai).